JOURNAL OF SCIENCE
SAKARYA UNIVERSITY

Sakarya University Journal of Science

ISSN 1301-4048 | e-ISSN 2147-835X | Period Bimonthly | Founded: 1997 | Publisher Sakarya University | http://www.saujs.sakarya.edu.tr/

Title: Influence of Top Layer Composition on the Photovoltaic Parameters of P3HT:PCBM Organic Solar Cells

Authors: Muhammet Erkan Köse
Recieved: 2019-04-04 12:00:27

Accepted: 2019-12-27 11:47:50

Article Type: Research Article
Volume: 24
Issue: 1
Month: February
Year: 2020
Pages: 257-264

How to cite
Muhammet Erkan Köse; (2020), Influence of Top Layer Composition on the Photovoltaic Parameters of P3HT:PCBM Organic Solar Cells . Sakarya University Journal of Science, 24(1), 257-264, DOI: 10.16984/saufenbilder.549216
Access link
http://www.saujs.sakarya.edu.tr/tr/issue/49430//549216

Sakarya University Journal of Science 24(1), 257-264, 2020

Influence of Top Layer Composition on the Photovoltaic Parameters of P3HT:PCBM Organic Solar Cells

Muhammet Erkan Köse[1]

Abstract

Spin and spray deposition techniques have been used sequentially to examine the effect of the composition of top blend layer on the photovoltaic properties of organic solar cells using well-known poly(3-hexylthiophene):[6,6]-Phenyl C61 butyric acid methyl ester (P3HT:PCBM) blend. Devices were prepared by spraying an extra layer of P3HT or PCBM (~15 nm) onto spin coated (1:1) blend film. P3HT-rich top phase slightly perturbs photovoltaic activity whereas PCBM-rich top phase drastically changes the power conversion efficiencies with a marked decrease in fill factors. While the annealed devices with P3HT-rich top phases display an average of 2.3% power conversion efficiencies, the same number drops to 1.5% in devices with PCBM-rich top phases in the active layer. Carrier mobilities were only marginally affected by the presence of spray coated top layers. However, series resistance of top phase P3HT-rich blends (~6 Ω/cm^2) remained the same with respect to spin coated sample whereas top phase PCBM-rich blends exhibit relatively higher series resistances for both annealed and non-annealed samples (~11 Ω/cm^2). Based on the presented results, one might speculate that electron injection to cathode with P3HT is almost as efficient as with PCBM for active layers utilizing P3HT:PCBM blend.

Keywords: organic photovoltaics, morphology, spray coating, P3HT, PCBM

1. INTRODUCTION

Organic photovoltaics (OPV) holds great promise to meet the demands for low cost photovoltaic technology due to solution processability and relatively cheaper organic materials utilized in the devices [1]. The major focus of OPV research is to increase the efficiency of devices by using novel materials with better photovoltaic activity. In a laboratory setting, spin-coating is the most common technique to deposit active layers during solar cell fabrication. However, it is clear that other types of coating techniques need to be used for large-area solar cells. In this regard, screen printing [2], doctor blading [3], and spray coating techniques [4] have been studied. Among these approaches, spray coating has been exploited by many research groups due to fast and economic deposition of organic-based layers [5, 6].

The power conversion efficiencies (PCEs) obtained with spray coating techniques are quite promising. For instance, Susanna et al. reported a device efficiency of 4.1% from a poly(3-

[1] Corresponding author: erkan.kose@kocaeli.edu.tr, ORCID: 0000-0003-3153-7436

hexylthiophene):[6,6]-Phenyl C61 butyric acid methyl ester (P3HT:PCBM) blend via airbrush coating [7]. Ultrasonic spray deposition has allowed much more uniform films with a PCE of 3.5% for the same blend [8]. In addition to the active layer, the hole transport layer poly (3,4-ethylenedioxythiophene):poly(styrene sulfonate (PEDOT:PSS) can be spray coated with device performances better or comparable to those of spin-coated devices [9, 10]. In general, the spray coated films display high surface roughness and less defined morphology, yet, fully spray coated devices operate as well as spin coated counterparts with long term device stability [9].

One salient feature of organic solar cells is the dependence of photovoltaic activity on blend morphology [11]. Controlling the bulk heterojunction (BHJ) morphology of active layer can lead to devices with improved photovoltaic properties. Spin coating technique helps little in control of morphological aspects of the blend layer. On the other hand, spray coating permits the deposition of layers by varying the blend composition of spray solution.

In general, it is believed that the inter-digitated donor and acceptor components with an acceptor-rich top phase and donor-rich bottom phase (Figure 1) are needed to achieve optimum photovoltaic activity in bulk heterojunction devices [1]. Here, we scrutinize this assumption by preparing and studying devices with varying vertical composition in the active layer. Our results show quite a different picture from what is assumed in this field in regards to ideal BHJ morphology of organic solar cells.

2. EXPERIMENTAL

Organic solar cells were fabricated on patterned indium tin oxide (ITO) glasses with a sheet resistance of 10-12 Ω/sq. The ITO glass was cleaned by sequential ultrasonic treatment in detergent, deionized water, acetone, and isopropanol, and then treated in a bench-top cleaner, The Plasma Etch, Inc., USA) for 2 min. PEDOT:PSS (Clevious P VP AI 4083 H. C.

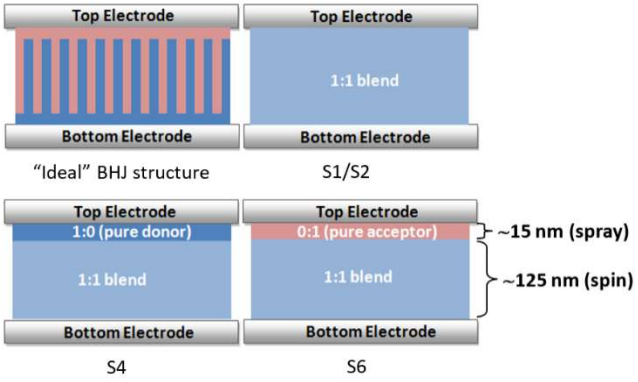

Figure 1. Vertical composition of BHJ devices studied in this work.

Stark, Germany) solution was filtered through a 0.45 µm filter and then spin coated at 4000 rpm for 60 s on the ITO electrode. Subsequently, the PEDOT:PSS layer was baked at 120 °C for 40 min in the air to remove any moisture that might be present in the film. The PEDOT:PSS coated substrates were transferred to a N_2 filled glovebox.

A blend solution of P3HT (Rieke Metals, Inc., MW = 17 kDa) and PCBM (Nano-C) in ortho-dichlorobenzene (1:1, w/w, 20 mg/mL) was filtered and then spin coated on top of PEDOT:PSS layer at 600 rpm for 30-60 s. After an hour of aging of the wet P3HT:PCBM blend films, the substrates were taken out of the glove box for spray deposition of the second layer. This extra layer was deposited by spray deposition using an airbrush at 20 psi N_2 gas pressure with 5 mg/mL P3HT or PCBM solutions prepared in chlorobenzene. Spray coated devices were then transferred to a nitrogen filled glove box. All of the device active layers were annealed once (unless otherwise noted) at 150 °C for 5 min on the hot plate in inert atmosphere. Then, the cathode consisting of LiF (~1 nm) capped with Al (~100 nm) was thermally evaporated on the active layer under a shadow mask in a base pressure of 2×10^{-6} mbar or better. The photovoltaic cells were encapsulated in the glove box with a UV-curable epoxy under glass sheets and then taken out for current density-voltage (J-V) measurements. The device active area was ~7.9 mm^2 for all the solar cells discussed in this work.

The J-V measurement of the devices was conducted on a computer controlled Keithley

2400 source meter. The J-V measurement system uses a solar simulator with a Class-A match to the AM1.5 Global Reference Spectrum. It is calibrated with KG5-filtered silicon reference cell with calibration traceable to NREL and NIST. Series resistances (R_s) of devices were estimated by using inverse of the slope at 1 V on J-V data under dark.

Optical micrograph and atomic force microscopy (AFM) images of the samples were recorded on a Veeco DI - 3100 atomic force micrometer. Film thicknesses of the blend films were measured with a Veeco (Dektak) step profiler. Scanning electron microscope (SEM) images were collected with JEOL JSM-6490LV system.

3. RESULTS AND DISCUSSION

Before discussing the results presented in this work, it is important to note that reported device performance parameters are the average of at least 18 devices (in some cases 24 devices). The spraying time as well as the distance between the airbrush and the sample was kept the same for all devices. Experimental procedure is strictly followed to maintain consistency among the device data. We first compare photovoltaic performance of fully spin coated and fully spray coated blends. Devices prepared by spin coating (S1) had higher device efficiencies compared to those prepared by spray coating (S2). In general, spray coated devices exhibited lower fill factor (FF) than those of spin coated analogues, indicating non-optimal blend morphology (Table 1). However, both open-circuit voltage (V_{OC}) and short-circuit density (J_{SC}) of spray coated devices are comparable to those of spin coated solar cells (Figure 2a). Figure 2b and 2c show the optical micrographs of spin coated and spray coated samples, respectively. The surface roughness of spray coated device is quite high whereas a smooth surface is obtained through spin coating, as expected [12]. However, AFM phase images show similar BHJ morphology on the surface (Figures 2d and 2e) of both films.

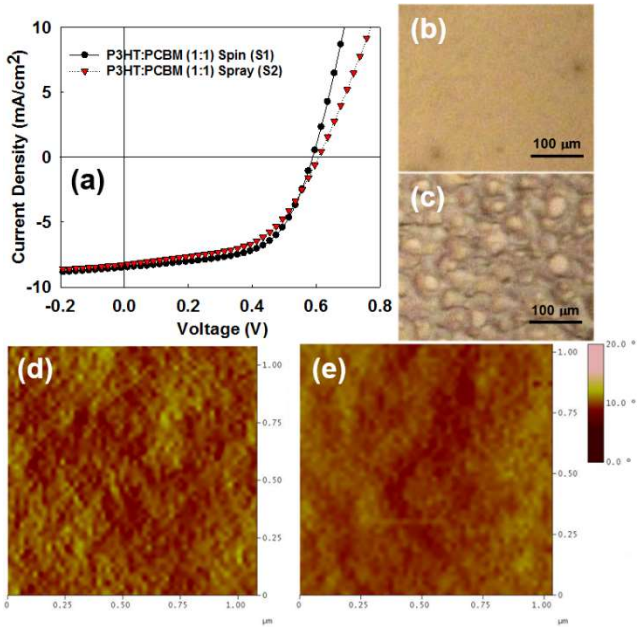

Figure 2. (a) J-V characteristics of the bulk-heterojunction P3HT:PCBM solar cells prepared by spin and spray coating techniques. Optical micrograph images of spin (b) and spray (c) coated films. AFM phase images of spin (d) and spray (e) coated samples.

In the next set of experiments, we sprayed an extra layer of P3HT or PCBM on a spin coated (1:1) blend film. In order to compare device parameters among different films, we kept the total film thickness around 140 ± 10 nm. Film thicknesses were monitored by a combination of step profiler and UV-vis spectroscopy measurements conducted on the films. The sprayed layer thickness was kept low around 15 ± 5 nm to ensure that 1:1 ratio of donor and acceptor components does not vary much from one device active layer to another. The reported exciton diffusion lengths of P3HT vary between 8 and 27 nm [13-15]. Therefore, the chosen extra layer is within the range where excitons created in such a layer have the opportunity to reach an acceptor molecule within their lifetime. To our knowledge, exciton diffusion length of PCBM is not reported, but parent acceptor, C_{60}, is known to have an exciton diffusion length of 30 - 35 nm [16]. Thus, the excitons formed in the sprayed layer should, in principle, contribute photocurrent generation.

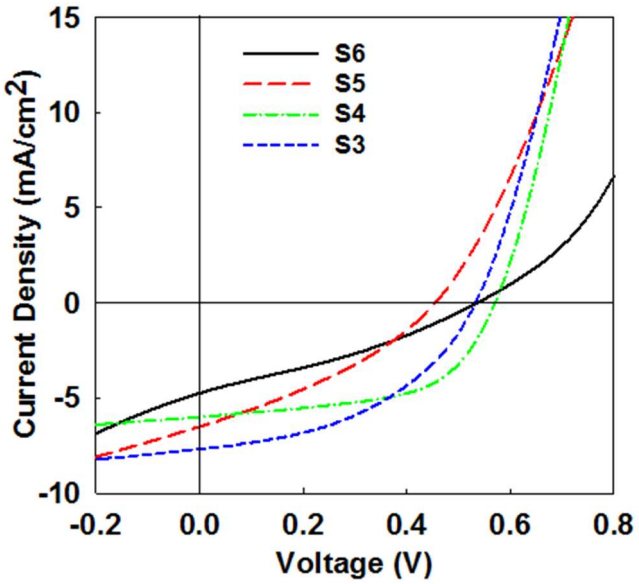

Figure 3. J-V characteristics of the bulk-heterojunction P3HT:PCBM solar cells with P3HT-rich and PCBM-rich top phases prepared by spray-coating at ambient conditions.

Figure 3 displays the J-V characteristics of top phase P3HT- or PCBM-rich solar cells under standard global AM1.5G solar conditions, and the corresponding photovoltaic data are listed in Table 1. We have examined both annealed and non-annealed devices after deposition of second layer with spray coating. The devices with P3HT-rich top phase exhibit similar solar cell characteristics to those of fully spray coated devices with a slight decrease in J_{SC}. However, annealed P3HT-rich device (S3) has a larger PCE than that of non-annealed (S4) analogue. In contrast, devices with PCBM-rich top phases display poor photovoltaic properties. Especially, non-annealed sample (S6) has significant decrease in J_{SC} and FF compared to the other device structures studied in this work.

The J-V diagram of S6 shows an inflection point (kink) [17]. Such behavior has been attributed to slow charge transfer at the electrical contact of absorber layer [18]. The fact that S3 and S4 devices do not exhibit such a behavior hints the high transport capability of holes and electrons for P3HT polymer at the active layer-electrode interfaces. FFs are considerably lower when cathode side of the blend layer is acceptor rich based on these results. Clearly, P3HT-rich top phase has slight effect on photovoltaic activity whereas PCBM-rich top phase drastically decreases the performance of solar cells.

Table 1. Average photovoltaic performance parameters of at least eighteen devices under simulated AM1.5G illumination at 100 mW / cm^2.

Sample (thickness)	P3HT:PCBM	V_{oc} (V)	J_{sc} (mA /cm^2)	FF (%)	PCE (%)
S1 (135 nm)	spin coated (1:1)	0.58 ± 0.01	8.4 ± 0.2	58.4 ± 2.2	2.9 ± 0.1
S2 (150 nm)	spray coated (1:1)	0.60 ± 0.01	8.2 ± 0.3	50.0 ± 2.5	2.4 ± 0.1
S3 (150 nm)	(1:1) spin + ~15 nm P3HT spray (annealed)	0.53 ± 0.01	7.7 ± 0.8	44.3 ± 4.9	2.3 ± 0.3
S4 (140 nm)	(1:1) spin + ~15 nm P3HT spray (w/o annealing)	0.57 ± 0.02	6.0 ± 0.7	57.0 ± 2.3	2.0 ± 0.2
S5 (130 nm)	(1:1) spin + ~10 nm PCBM spray (annealed)	0.45 ± 0.07	6.5 ± 0.9	40.4 ± 11.0	1.5 ± 0.6
S6 (138 nm)	(1:1) spin + ~15 nm PCBM spray (w/o annealing)	0.54 ± 0.05	4.7 ± 0.9	36.0 ± 12.5	0.9 ± 0.5

To further reveal the effect of spray coated films on device photovoltaic responses; we have measured the series resistance and the carrier mobilities of each sample (Table 2). Space-charge limited current (SCLC) method has been used to measure carrier mobilities [19, 20]. For hole-only devices Al/active layer/Al device architecture and for electron-only devices ITO/PEDOT:PSS/active layer/MoO_3/Al device configuration have been used. P3HT has higher hole mobility (4.4×10^{-4} cm^2/V·s) than its electron mobility (1.6×10^{-4} cm^2/V·s) with this setup, in accordance with previous experimental observations [21]. Carrier mobilities for the P3HT:PCBM active layer in S1 and S2 are on the order of 10^{-4} cm^2/V·s, though latter has higher electron mobility than its hole mobility. Despite the fact that S2 has been prepared by spray coating method, the magnitude of its carrier mobilities are very similar to those of S1 sample,

which have been deposited using traditional spin coating. All the other samples have also carrier mobilities on the order of 10^{-4} $cm^2/V{\cdot}s$. The carrier mobility ratio, μ_h / μ_e, is relatively larger for holes P3HT rich top layer (S3 and S4) devices whereas the same ratio is smaller for PCBM rich top layer devices (S5 and S6). This is expected considering the vertical composition of each active layer. One striking feature is that whether the device has P3HT rich top phase or PCBM rich phase, the carrier mobilities are not severely affected by the top layer composition. This manifests itself as rather decent device efficiencies obtained for S3-6 samples.

Table 2. Series resistance (R_s), hole (μ_h) and electron (μ_e) mobilities of the devices studied in this work.

Sample	μ_h ($cm^2/V{\cdot}s$) / 10^{-4}	μ_e ($cm^2/V{\cdot}s$) / 10^{-4}	μ_h / μ_e	R_s (Ω/cm^2)
P3HT only	4.4	1.6	2.8	-
S1	2.7	1.8	1.5	6.8
S2	2.3	3.3	0.7	14.0
S3	4.0	2.2	1.8	6.6
S4	4.3	0.8	5.4	5.0
S5	4.9	3.0	1.6	11.0
S6	3.6	2.8	1.3	11.5

The series resistances of S3 and S4 are very similar to that of spin coated sample (S1). That means the presence of extra amount of P3HT on top does not increase the series resistance. However, PCBM rich top layer devices exhibit rather large series resistance, which partially explains the relatively lower device efficiencies recorded for S5 and S6 samples. It looks like annealing has no influence on series resistance (compare S3 vs. S4 or S5 vs. S6). This observation suggest unchanging morphologies and poor mixing of spin coated and spray coated layers when extra P3HT or PCBM is introduced on top of spin coated film, as will be further supported by the imaging results below. One notable difference between R_s of S1 and S2 is that series resistance of S2 is quite large. Such difference can be attributed to non-optimal blend morphology for spray coated devices. It is well-known that large series resistance causes drops in FF, which is also the case for S2.

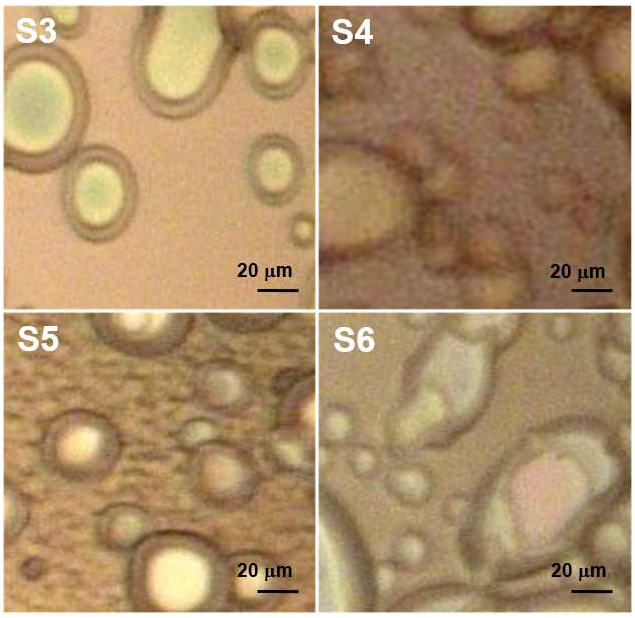

Figure 4. Optical micrograph images of the films for S3, S4, S5, and S6 samples.

Optical micrographs collected on S3, S4, S5, and S6 samples show the existence of little droplets on spin coated bottom layer (Figure 4). Annealed films (S4 and S6) have hazy images due to probably slightly better mixing and reorganization of droplets with the bottom spin coated layer. Earlier reports suggest formation of P3HT:PCBM BHJ structure within a few seconds of annealing at 150 °C [22]. However, the droplets still maintain their structural features after the annealing process. To further understand the interface between the spin coated bottom layer and spray coated top layer, SEM images were collected on a sample substrate. A representative image for heavily P3HT sprayed top layer (with a thickness of 140 nm) has been given in Figure 5. SEM image clearly shows distinct two different phases even after annealing the sample at 150 °C for 5 min. That is, general structural features of both top layer and bottom layer are preserved whether annealing has been performed or not for the active layer in question. However, this is valid only for a thick spray coated layer sitting on a spin coated film. A very thin layer of (~15 nm) P3HT and PCBM spray coated layer can mix with the bottom layer well. Our efforts to visualize such small thicknesses in S3-6 samples did not allow unambiguous identification of each layer, possibly due to the limitations in the clarity of the images.

To further test the effect of top layer composition on device performances, we sprayed a large amount of P3HT onto spin coated blend, achieving a total blend layer thickness of ~600 nm. J-V measurements on annealed samples of such a thick film gave a PCE = 1.91%, J_{SC} = 6.05 mA/cm^2, V_{OC} = 0.56 V, and FF = 56%. In contrast, when an extra ~100 nm PCBM is sprayed onto spin coated film, device efficiencies drop as low as 0.25% with poor fill factors around 30 percent. Evidently, a large amount of donor P3HT material on top of spin coated film does not change photovoltaic activity in contrast to common expectations. However, accumulation of large amount of PCBM on the cathode side clearly has severe consequences on device operation.

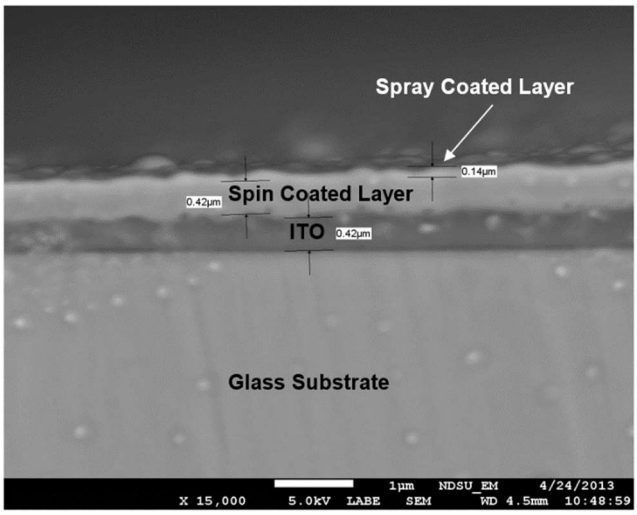

Figure 5. SEM cross-sectional image of spin and spray coated layers on a sample ITO coated glass substrate. Note that a large amount of P3HT has been sprayed on top of spin coated film to better visualize each layer.

These results suggest that the 'ideal' BHJ morphology for P3HT:PCBM based solar cells does not necessarily require a vertical active layer composition as depicted in Figure 1. The recorded device parameters also indicate P3HT has significant role in electron injection to cathode and PCBM is not absolutely required for efficient charge injection at the active layer-cathode interface. The existence of a thin-layer of electron-rich P3HT next to the cathode may alter the work function of the cathode via affecting surface dipoles [23]. Such surface dipoles could decrease the electron injection barrier height, and thereby facilitate efficient electron extraction, which in turn influence solar cell device performance [24]. It is important to note that well-known band diagram of above mentioned devices justify the conclusion above, though this may be only valid for solar cells using P3HT:PCBM blend as active layer. Other blends may exhibit different photovoltaic properties based on active layer morphology and the vertical composition of donor and acceptor materials within the film.

4. CONCLUSIONS

In summary, spray coating techniques allow deposition of active layers with possible control on vertical composition of blend layer in organic solar cells. However, acceptor-rich top phase is detrimental to photocurrent generation in P3HT:PCBM BHJ solar cells. J_{SC} and, in particular, FFs adversely affected from such a distribution of blend components. Series resistances of devices increase substantially in active layers with PCBM rich top phase. Therefore, it is of the utmost importance not to use PCBM rich top phases in the blend of the active layer which in turn can limit the photovoltaic activity in organic solar cells. The presented results also emphasize the need to re-evaluate the 'ideal' bulk heterojunction morphology accepted by many scientists in organic solar cell research, at least for devices exploiting P3HT:PCBM blend in the active layer.

5. REFERENCES

[1] S. Gunes, H. Neugebauer, and N. S. Sariciftci, "Conjugated polymer-based organic solar cells," Chemical Reviews, vol. 107, pp. 1324-1338, 2007.

[2] S. E. Shaheen, R. Radspinner, N. Peyghambarian, and G. E. Jabbour, "Fabrication of bulk heterojunction plastic solar cells by screen printing," Applied Physics Letters, vol. 79, pp. 2996-2998, 2001.

[3] P. Schilinsky, U. Asawapirom, U. Scherf, M. Biele, and C. J. Brabec, "Influence of the molecular weight of poly(3-hexylthiophene) on the performance of bulk heterojunction solar cells," Chemistry of Materials, vol. 17, pp. 2175-2180, 2005.

[4] R. Green, A. Morfa, A. J. Ferguson, N. Kopidakis, G. Rumbles, and S. E. Shaheen, "Performance of bulk heterojunction photovoltaic devices prepared by airbrush spray deposition," Applied Physics Letters, vol. 92, 033301, 2008.

[5] C. Girotto, D. Moia, B. P. Rand, and P. Heremans, "High-Performance Organic Solar Cells with Spray-Coated Hole-Transport and Active Layers," Advanced Functional Materials, vol. 21, pp. 64-72, 2011.

[6] H. Y. Park, K. Kim, D. Y. Kim, S. K. Choi, S. M. Jo, and S. Y. Jang, "Facile external treatment for efficient nanoscale morphology control of polymer solar cells using a gas-assisted spray method," Journal of Materials Chemistry, vol. 21, pp. 4457-4464, 2011.

[7] G. Susanna, L. Salamandra, T. M. Brown, A. Di Carlo, F. Brunetti, and A. Reale, "Airbrush spray-coating of polymer bulk-heterojunction solar cells," Solar Energy Materials and Solar Cells, vol. 95, pp. 1775-1778, 2011.

[8] K. X. Steirer, M. O. Reese, B. L. Rupert, N. Kopidakis, D. C. Olson, R. T. Collins, and D. S. Ginley, "Ultrasonic spray deposition for production of organic solar cells," Solar Energy Materials and Solar Cells, vol. 93, pp. 447-453, 2009.

[9] S. F. Tedde, J. Kern, T. Sterzl, J. Furst, P. Lugli, and O. Hayden, "Fully Spray Coated Organic Photodiodes," Nano Letters, vol. 9, pp. 980-983, 2009.

[10] J. Weickert, H. Y. Sun, C. Palumbiny, H. C. Hesse, and L. Schmidt-Mende, "Spray-deposited PEDOT:PSS for inverted organic solar cells," Solar Energy Materials and Solar Cells, vol. 94, pp. 2371-2374, 2010.

[11] A. Pivrikas, H. Neugebauer, and N. S. Sariciftci, "Influence of processing additives to nano-morphology and efficiency of bulk-heterojunction solar cells: A comparative review," Solar Energy, vol. 85, pp. 1226-1237, 2011.

[12] C. N. Hoth, R. Steim, P. Schilinsky, S. A. Choulis, S. F. Tedde, O. Hayden, and C. J. Brabec, "Topographical and morphological aspects of spray coated organic photovoltaics," Organic Electronics, vol. 10, pp. 587-593, 2009.

[13] P. E. Shaw, A. Ruseckas, and I. D. W. Samuel, "Exciton diffusion measurements in poly(3-hexylthiophene)," Advanced Materials, vol. 20, pp. 3516-3520, 2008.

[14] M. E. Kose, P. Graf, N. Kopidakis, S. E. Shaheen, K. Kim, and G. Rumbles, "Exciton Migration in Conjugated Dendrimers: A Joint Experimental and Theoretical Study," ChemPhysChem, vol. 10, pp. 3285-3294, 2009.

[15] S. Cook, L. Y. Han, A. Furube, and R. Katoh, "Singlet Annihilation in Films of Regioregular Poly(3-hexylthiophene): Estimates for Singlet Diffusion Lengths and the Correlation between Singlet Annihilation Rates and Spectral Relaxation," Journal of Physical Chemistry C, vol. 114, pp. 10962-10968, 2010.

[16] D. S. Qin, P. Gu, R. S. Dhar, S. G. Razavipour, and D. Y. Ban, "Measuring the exciton diffusion length of C-60 in organic planar heterojunction solar cells," Physica Status Solidi a-Applications and Materials Science, vol. 208, pp. 1967-1971, 2011.

[17] B. Romero, G. del Pozo, and B. Arredondo, "Exact analytical solution of a two diode circuit model for organic solar cells showing S-shape using Lambert W-functions," Solar Energy, vol. 86, pp. 3026-3029, 2012.

[18] M. Glatthaar, M. Riede, N. Keegan, K. Sylvester-Hvid, B. Zimmermann, M. Niggemann, A. Hinsch, and A. Gombert, "Efficiency limiting factors of organic bulk heterojunction solar cells identified by electrical impedance spectroscopy," Solar Energy Materials and Solar Cells, vol. 91, pp. 390-393, 2007.

[19] Z. H. Lin, J. Bjorgaard, A. G. Yavuz, A. Iyer, and M. E. Kose, "Synthesis, photophysics, and photovoltaic properties of low-band gap conjugated polymers based on thieno 3,4-c pyrrole-4,6-dione: a combined experimental and computational study," Rsc Advances, vol. 2, pp. 642-651, 2012.

[20] C. Goh, R. J. Kline, M. D. McGehee, E. N. Kadnikova, and J. M. J. Frechet, "Molecular-weight-dependent mobilities in regioregular poly(3-hexyl-thiophene) diodes," Applied Physics Letters, vol. 86, 122110, 2005.

[21] S. A. Choulis, Y. Kim, J. Nelson, D. D. C. Bradley, M. Giles, M. Shkunov, and I. McCulloch, "High ambipolar and balanced carrier mobility in regioregular poly(3-hexylthiophene)," Applied Physics Letters, vol. 85, pp. 3890-3892, 2004.

[22] D. Chen, F. Liu, C. Wang, A. Nakahara, and T. P. Russell, "Bulk Heterojunction Photovoltaic Active Layers via Bilayer Interdiffusion," Nano Letters, vol. 11, pp. 2071-2078, 2011.

[23] I. G. Hill, A. Rajagopal, A. Kahn, and Y. Hu, "Molecular level alignment at organic semiconductor-metal interfaces," Applied Physics Letters, vol. 73, pp. 662-664, 1998.

[24] N. Koch, S. Duhm, J. P. Rabe, S. Rentenberger, R. L. Johnson, J. Klankermayer, and F. Schreiber, "Tuning the hole injection barrier height at organic/metal interfaces with (sub-) monolayers of electron acceptor molecules," Applied Physics Letters, vol. 87, 101905, 2005.